



DOI: doi.org/10.21009/SPEKTRA.071.02

CHARACTERIZATION OF $(\text{Mg}_{0.6}\text{Zn}_{0.4})\text{TiO}_3$ CERAMICS AS DIELECTRIC RESONATOR MATERIALS IN MICROWAVE FREQUENCIES

Syah N. M. Ishak, Frida U. Ermawati*

Department of Physics, Faculty of Mathematics and Natural Sciences, Universitas Negeri Surabaya, Surabaya 60231, Indonesia

*Corresponding Author Email: frida.ermawati@unesa.ac.id

Received: 1 April 2022
Revised: 27 April 2022
Accepted: 28 April 2022
Online: 29 April 2022
Published: 30 April 2022

SPEKTRA: Jurnal Fisika dan Aplikasinya
p-ISSN: 2541-3384
e-ISSN: 2541-3392



ABSTRACT

Ceramics based on magnesium titanate (MgTiO_3) are dielectric materials that have the potential to be used in telecommunications systems at microwave frequencies, such as filters, antennas, and signal generators. This study aims to characterize the resonant frequency and output power of $(\text{Mg}_{0.6}\text{Zn}_{0.4})\text{TiO}_3$ ceramics (abbreviated MZT04) as a dielectric resonator (DR) material in a DRO circuit and relate it to the structure, microstructure, and bulk density data of the ceramics. The MZT04 ceramics were fabricated by compacting MZT04 powder at a pressure of 2.5 MPa using a cylindrical die press of 5 mm in diameter to become pellets with the same diameter. The pellets were sintered at 1300°C by varying holding time for 6, 8, and 10 h to become ceramics. Data on the structure of the ceramics were obtained from the X-Ray Diffraction (XRD) pattern with Cu-K α radiation which showed that the three ceramics contained MgTiO_3 phase, each 87.02; 90.55; and 87.40 % molar, the rest % is MgO and TiO_2 rutile phases. The increase in sinter holding time has increased the unit cell volume of the MgTiO_3 phase from (307.94), (308.61), to (308.94) Å³; the size of the lattice parameters (a=b, c) also increased from (5.057, 13.903) Å, (5.058, 13.903) Å, to (5.061, 13.914) Å; like wise, the bulk density increased from 2.51, 2.82, and 3.04 g/cm³. As a DR material, the three ceramics exhibit a resonant frequency signal each at 5.20; 5.21; and 5.22 GHz with the output power of -19.70; -14.47; -15.70 dBm, and the FWHM of the signal is 59.3; 61.6; and 61.2 MHz. Therefore, MZT04 ceramics can be applied as the DR material in microwave frequencies, especially at ~5.20 GHz. The variations in sinter holding time is not significant effect on the position of the resonant frequency.

Keywords: $(\text{Mg}_{0.6}\text{Zn}_{0.4})\text{TiO}_3$ ceramic, resonant frequency, dielectric resonator material, structure, microstructure

INTRODUCTION

Magnesium titanate (MgTiO_3) ceramic is a dielectric material that plays an important role in microwave communications systems like filters, antennas, multilayer capacitors, and signal generators [1]–[8]. The ceramics have superior dielectric properties, such as high-quality factor ($Q < 20000$ at 8GHz) and medium dielectric constant ($\epsilon_r = 17$) so that they can be used as a material of a dielectric resonator oscillator (DRO) [9], [10]. DRO is a circuit of microstrip lines coupled with a dielectric material that acts as a resonator (see FIGURE 1) [11]–[14]. DRO is also one of the oscillators that have a Q value and high-temperature stability [15]. DRO has a constant dielectric value between 20 and 80, which can operate up to 100 GHz [16]. Dimensions of DRO will be large when used at a low working frequency [17]. FIGURE 2 shows a block diagram for measuring the resonant frequency of a DR material, where the DRO box in FIGURE 2 is the DRO circuit in FIGURE 1 which consists of 4 components. The DRO box was connected to a spectrum analyzer and a power supply. FIGURE 3 shows the dimensions and the equivalence circuit of the DRO material used in FIGURE 1.

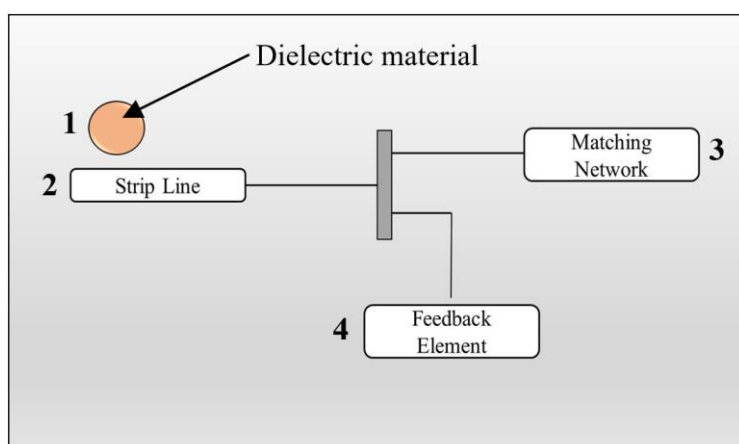


FIGURE 1. DRO circuit consists of 4 components: 1, 2, 3, and 4 [18]

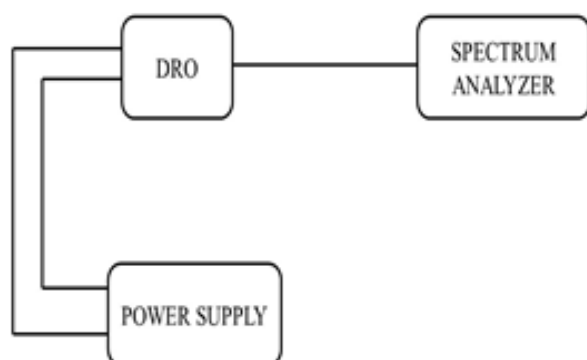


FIGURE 2. DRO block diagram [18]

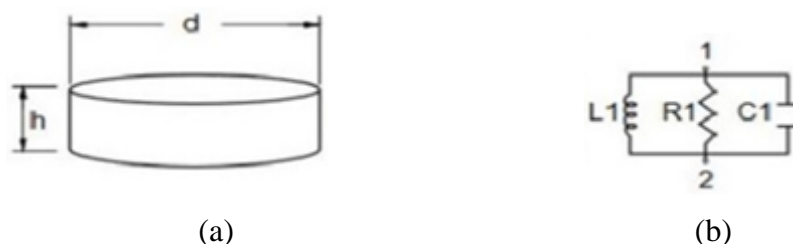


FIGURE 3. a) Dimensions of a ceramic material used as DRO material in FIGURE 1; b) and its equivalent circuit [19]

In FIGURE 1, as already explained, the DRO circuit consists of 4 components, i.e: 1) dielectric material, 2) strip line, 3) matching network and 4) feedback element. The dielectric material is a ceramic which acts as a resonator and has dimensions as shown in FIGURE 3a. Meanwhile, DRO also has a replacement circuit in the form of resistors, inductors, and capacitors which parallel connected (see FIGURE 3b). The working principle and function of the dielectric material as a resonator are similar to that of the resonator cavity [20]. Microwaves stored in the resonator material will supply the permittivity value on the resonator's surface, and microwaves will bounce back between the sides of the resonator wall [21]. DRO can work in transverse electrical (TE) mode [22]–[24]. The TE mode is an electric wave that propagates in a rectangular waveguide. The TE mode that is often used is TE_{0.18}. The resulting resonant frequency in the TE_{0.18} mode can be deduced using EQUATION (1) [25].

$$f_o(\text{GHz}) = \frac{8.533}{\sqrt{\epsilon_r \left(\frac{\pi}{4} d^2 h\right)^{1/3}}} \quad (1)$$

Where d is the diameter of the resonator (mm), h is the thickness of the resonator (mm) and ϵ_r is the dielectric constant of the resonator.

MgTiO₃-ceramic fabrication has been reported by several authors, one of them by Zhang et al. [2] that fabricated (Mg_{0.97}M_{0.03})TiO₃ ceramics for M = Ni, Zn, Co, and Mn and sintered at 1275 °C for 4h. The ceramic with M = Zn, namely (Mg_{0.97}Zn_{0.03})TiO₃, MgTiO₃ phase was identified as the pure phase. Further, Kadarosman & Ermawati [21] that fabricated (Mg_{0.9}Zn_{0.1})TiO₃ ceramics by adding to 2 wt.% Bi₂O₃ and sintered at 1000, 1100, and 1200°C for 4 h. It was reported by Kadarosman & Ermawati [21] that the MgTiO₃ phase was detected as the main phase of (93.63±2.15) % molar at 1000°C, (93.83±1.92) % molar at 1100°C, and (90.78±1.89) % molar at 1200 °C. The rest molar % is the MgTi₂O₅ phase. Furthermore, Wang et al. [26] that fabricated (0.95MgTiO₃-0.05CaTiO₃) ceramics and sintered at 1200, 1300, and 1400°C for 4h. It was reported by Wang et al. [26] that the MgTiO₃ phase was detected as the main phase for all sinter temperatures accompanied with the CaTiO₃ phase. Moreover, Ermawati et al. [27] that fabricated (Mg_{1-x}Zn_x)TiO₃ ceramics for x = 0; 0.1; 0.2; 0.3; 0.4; 0.5 and sintered at 1400°C for 8 h. For ceramic with x = 0.4, namely (Mg_{0.6}Zn_{0.4})TiO₃, i.e. the same ceramic as the ceramic reported in this work, the MgTiO₃ phase was identified as the main phase (82 % vol.) accompanied with Zn₂TiO₄ phase. Ermawati et al. [27] reported that Zn₂TiO₄ is another ceramic material that is more conductive when compared to

$(\text{Mg}_{0.6}\text{Zn}_{0.4})\text{TiO}_3$, so its presence in $(\text{Mg}_{0.6}\text{Zn}_{0.4})\text{TiO}_3$ ceramic system could be detrimental because it tended to reduce the dielectric properties of the parent ceramic. However, Ermawati et al [27] have not reported the potential use of $(\text{Mg}_{0.6}\text{Zn}_{0.4})\text{TiO}_3$ ceramic as a dielectric resonator material.

Therefore, this study reports the work to fabricate $(\text{Mg}_{0.6}\text{Zn}_{0.4})\text{TiO}_3$ ceramics (abbreviated MZT04) without accompanied with Zn_2TiO_4 phase. The aim was to characterize the potential of the MZT04 ceramics as resonator materials in DRO circuits at microwave frequencies. The discussion is carried out using the structure, microstructure, and bulk density data of the ceramics. The ceramics were sintered at 1300°C by varying holding time of 6, 8, and 10 h.

METHOD

Ceramic Fabrication

The MZT04 powder that was synthesized by Ermawati et al. [27] using the solution mixing method from high purity metal powders of as the starting materials were used in this work to fabricate the ceramics. In this work, the fabrication of MZT04 ceramics was carried out by compacting the MZT04 powder above using the 5-mm diameter of a cylindrical die press & a hydraulic hand press. The applied pressure was 2.5 MPa for 10 s. The 2.5 MPa pressure was chosen according to the recommendations given by Kadarosman & Ermawati [21], where the resulting resonant frequency was 5.11 GHz even for fabrication $(\text{Mg}_{0.9}\text{Zn}_{0.1})\text{TiO}_3$ ceramics. In this work, the MZT04 ceramics were sintered at 1300°C for 6, 8, and 10 h.

Ceramic Characterization

The structure data was obtained from X-Ray Diffraction (XRD) patterns which were measured using Bragg-Brentano Philips X'pert Diffractometer, with $\text{Cu-K}\alpha$ radiation, 2θ range = $15-70^\circ$ and the step size = $0.02^\circ/\text{min}$. Analysis of the XRD patterns was carried out qualitative and quantitatively. The qualitative analysis was carried out using Match! Software to identify any crystalline phases in MZT04 ceramics. The quantitative analysis was carried out by the Rietveld method using Rietica software to extract the lattice parameter, % molar, and unit cell volume data of all identified phases. Microstructural data that was taken from a broken surface of each ceramics was identified using a scanning electron microscope (SEM) FEI inspects S50 with a magnification of 5000x and operating at 20 kV. The average grain and pore diameter sizes on the microstructures were analyzed using ImageJ software. FIGURE 4 demonstrates the measurement of the average grain diameter on the MZT04 ceramics.

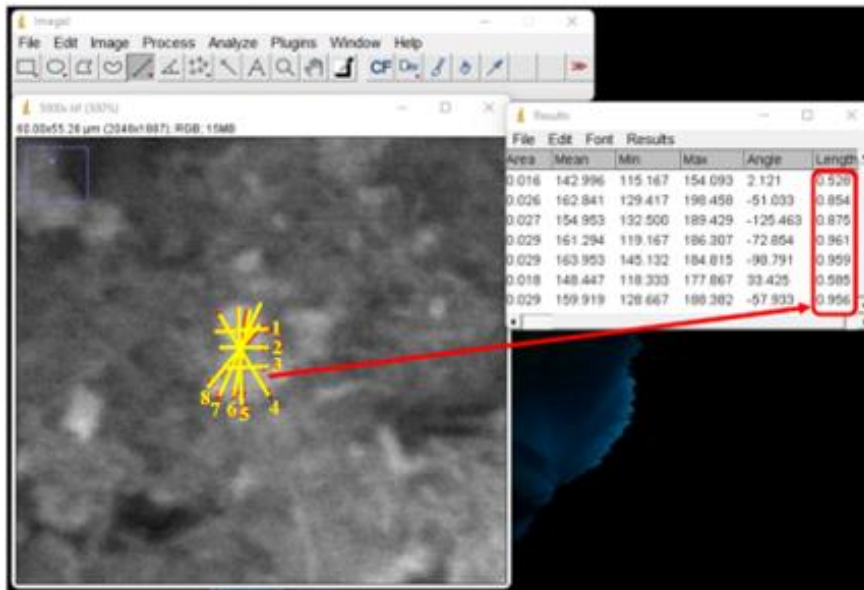


FIGURE 4. A demonstration of measuring an average diameter of a grain using ImageJ software from different positions (No. 1-8) due to the asymmetrical shape of the grain. Inset table: the measured grain diameters from the 8 different positions, i.e. the “length” column.

The bulk density of MZT04 ceramics was measured with the Archimedes method integrated to HyperTerminal software using EQUATION (2) [28].

$$\rho = \frac{m_d}{m_w + m_a} \rho_a \quad (2)$$

Where ρ is a bulk density of the ceramic (g/cm^3), m_d is the dry mass of ceramic (g), m_a is the Archimedes mass (g), m_w is the wet mass of ceramic (g), and ρ_a is the density of aquadest (g/cm^3) as the medium. The resonant frequency of the ceramics in the DRO circuit was measured using a spectrum analyzer (Keysight MXA Signal Analyzer N9020A) operating in TE₀₁₈ mode within 3-12 GHz, 9-12 Volt, and 100-200 mA. FIGURE 5 shown a set up experiment to measure the resonant frequency of MZT04 ceramic in the DRO circuit.

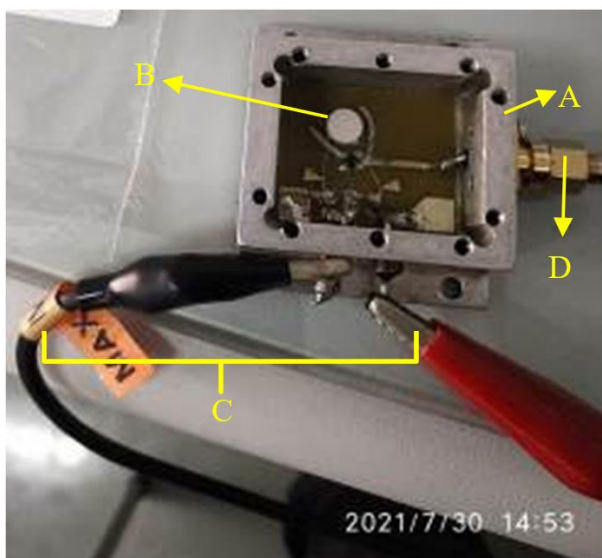


FIGURE 5. The MZT04 ceramic resonant frequency measurement as a DR material in a DRO circuit.

In FIGURE 5, The set up experiment consists of 4 main components, namely A, B, C, and D, where A = the square box = DRO circuit as described in the Introduction section, B = MZT04 ceramic as a DR material, C = 2 types of connector (black and red) to connect A to the power supply and D = the connector that connects A to the spectrum analyzer.

RESULT AND DISCUSSION

Structure

FIGURE 6 shown the XRD patterns of the three MZT04 ceramics measured using a Bragg-Brentano Philips X'pert Diffractometer, with Cu-K α radiation, 2θ range = 15-70°, and the step size = 0.02 °/min. The phase identification on the patterns in FIGURE 6 was carried out using the Match! Software. FIGURE 7 shows the results of the refinement of the three XRD patterns in FIGURE 6 using the Rietveld method and Rietica software. TABLE 1 summarizes the results of refinement using the Rietveld method for the three patterns in FIGURE 7 consisting of % molarity, lattice parameters, and unit cell volume for all identified phases.

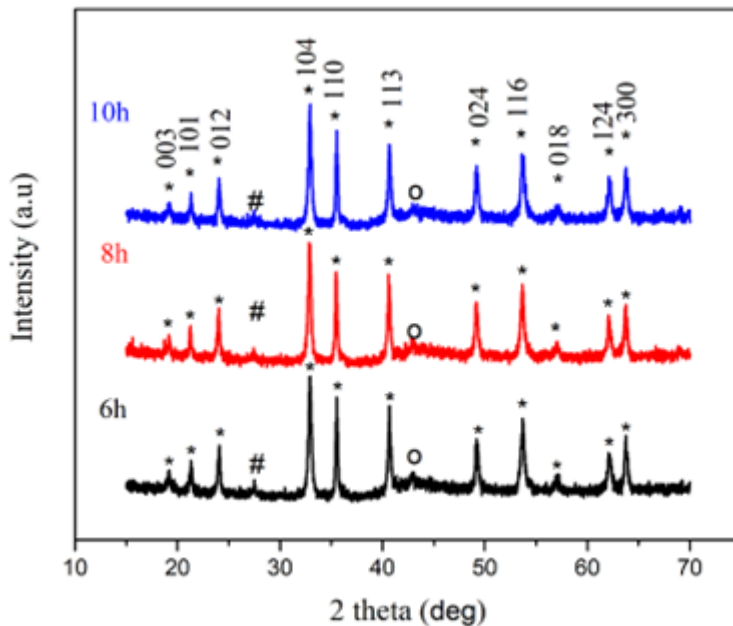
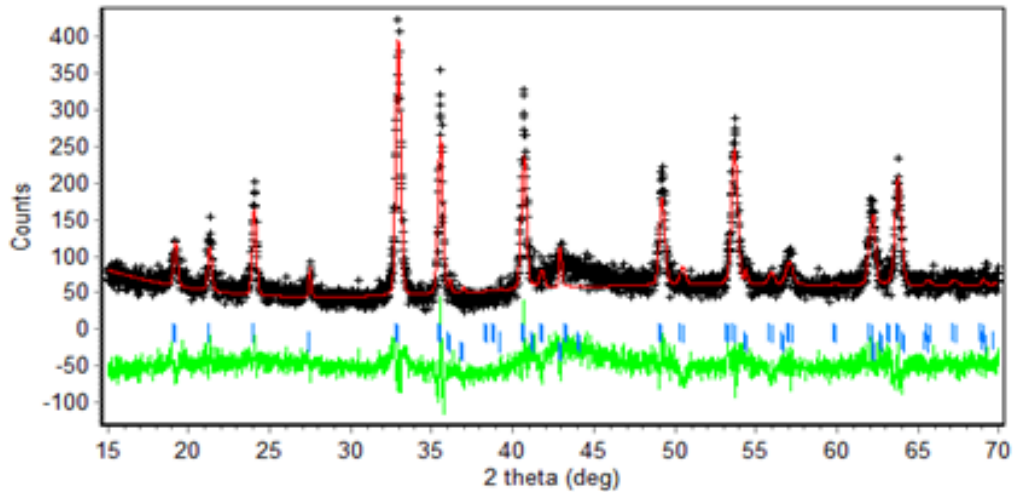
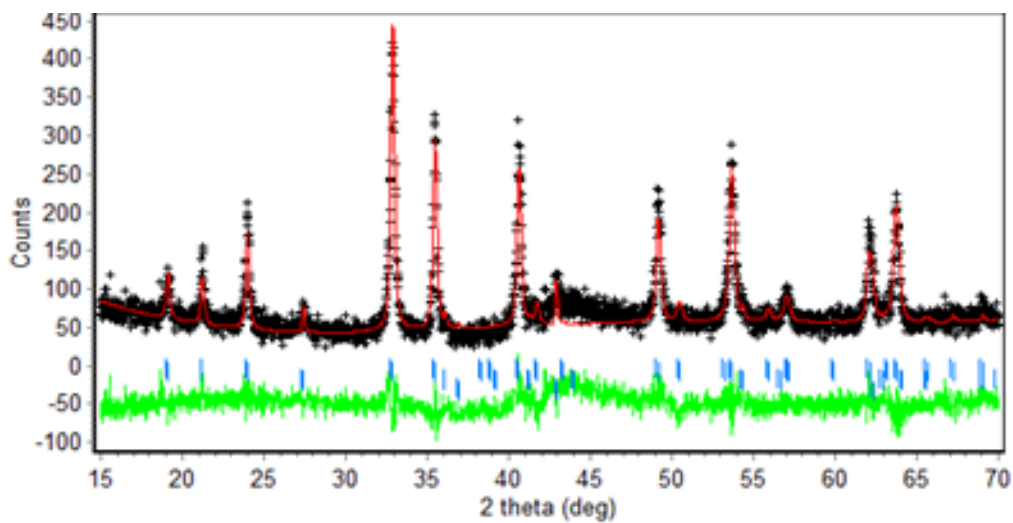


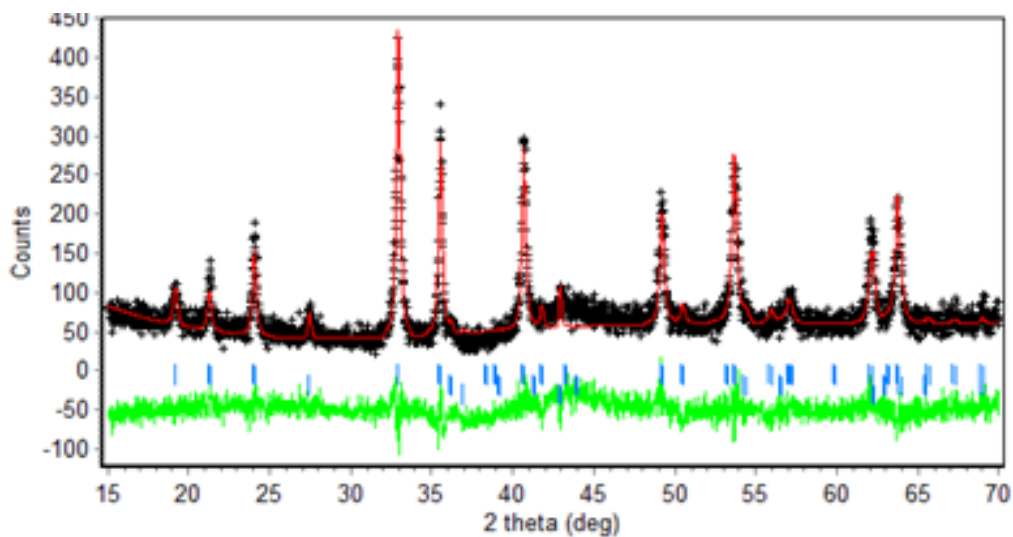
FIGURE 6. The XRD patterns of the MZT04 ceramics sintered at 1300 °C for 6, 8, and 10 h, Symbol * = MgTiO₃ (PDF No. 06-0494), # = TiO₂ rutile (PDF No. 21-2176), o = MgO (PDF No. 45-0946).



(a)



(b)



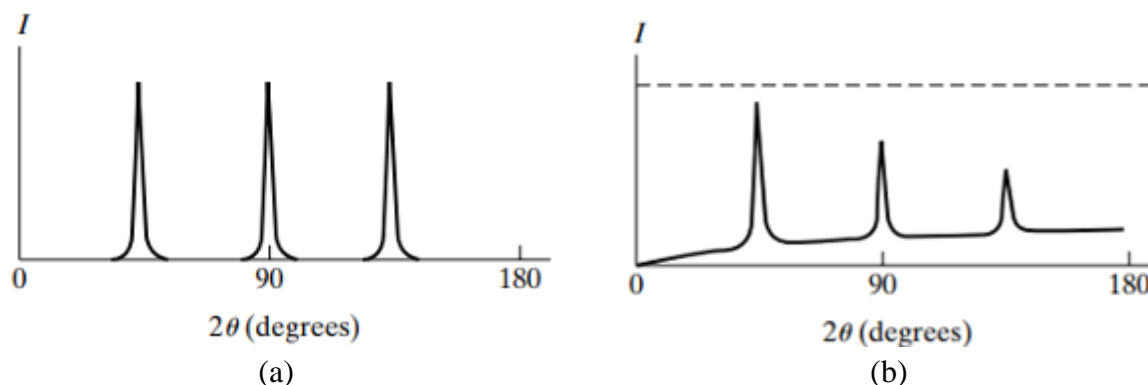
(c)

FIGURE 7. The rietveld refinement of the XRD patterns in Figure 6 for (a) 6 h, (b) 8 h, (c) 10 h, (a) FoM = 2.206; $R_p = 13.69$; $R_{wp} = 17.51$; $R_{exp} = 11.79$, (b) FoM = 2,047; $R_p = 13.00$; $R_{wp} = 16.92$; $R_{exp} = 11.83$, (c) FoM = 1.962; $R_p = 12.88$; $R_{wp} = 16.56$; $R_{exp} = 11.82$.

TABLE 1. The output of Rietveld refinement on FIGURE 7 consists of % molar, lattice parameters, and unit cell volume of the three MZT04 ceramics.

MZT04 ceramics, 1300 °C	Identified phase	Lattice parameters (Å)	Unit cell volume (Å ³)	% Molar
6 h	MgTiO ₃	a=b 5.057 c 13.903	307.94±0.08	87.02±2.01
	TiO ₂	a=b 4.592 c 2.961	62.46±0.06	12.96±1.22
	MgO	a=b=c 4.216	74.94±0.03	0.02±0.00
8 h	MgTiO ₃	a=b 5.058 c 13.900	308.01±0.08	90.55±2.23
	TiO ₂	a=b 4.956 c 2.956	62.44±0.07	9.44±1.03
	MgO	a=b=c 4.213	74.80±0.03	0.02±0.00
10 h	MgTiO ₃	a=b 5.061 c 13.914	308.94±0.12	87.40±2.74
	TiO ₂	a=b 4.607 c 2.953	62.69±0.12	12.58±1.79
	MgO	a=b=c 4.220	75.17±0.04	0.02±0.00

Before discussing FIGURE 6-7, and TABLE 1 in detail, we will first discuss the phenomenon of the increase in the background spectrum at $2\theta = 40-70^\circ$ in FIGURE 6. The increase in the background may be closely related to the high sintering temperature (1300 °C) which was applied to the MZT04 ceramics. According to Cullity & Stock [29], this phenomenon was due to the atom's thermal vibrations, which can result in a decrease in the intensity of diffraction and scattering in all directions which is called temperature diffuse scattering (TDS) as shown in FIGURE 8.

**FIGURE 8.** The comparison of the diffraction pattern (hypothetical pattern) between: (a) without the TDS phenomenon and (b) the presence of the TDS phenomenon due to the high heating temperature of the sample [29].

In FIGURE 8a, the hypothetical pattern of atoms at rest (atoms are not subjected to thermal vibration due to heating temperature is not high). The hypothetical pattern consists of three peaks with the same distance and intensity and without a background. Meanwhile, FIGURE 8b shows the same peaks as FIGURE 8a but the intensity is reduced by a factor of e^{-2m} and at the same time the peak intensity is 'corrupted' by the background due to the TDS phenomenon. The TDS phenomenon was observed when one of the three XRD patterns in FIGURE 6 was compared with the XRD pattern of the same ceramic but sintered at 1100°C for 2 h (see FIGURE 9).

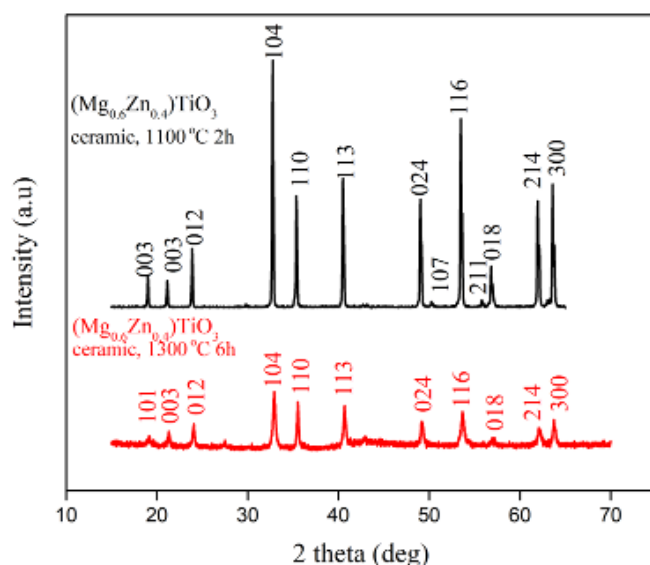


FIGURE 9. The comparison of XRD patterns intensity and background in $(\text{Mg}_{0.6}\text{Zn}_{0.4})\text{TiO}_3$ ceramic reported in [30] without TDS Phenomenon versus those of $(\text{Mg}_{0.6}\text{Zn}_{0.4})\text{TiO}_3$ ceramic examined in this present study.

In FIGURE 9, the intensity of the diffraction peaks when the ceramic was sintered at 1100°C is much higher than when sintered at 1300°C . In addition, the increase in the background in FIGURE 9 was visible at $2\theta = 40-70^\circ$. This is an indication of the TDS phenomenon that occurs in the $(\text{Mg}_{0.6}\text{Zn}_{0.4})\text{TiO}_3$ ceramics in this study.

Returns to FIGURES 6-7, and TABLE 1. In FIGURE 6, the peaks with '*' and Miller indices correspond to the diffraction peaks belonging to the MgTiO_3 phase (PDF No. 06-0494). The minor peak with '#' corresponds to the TiO_2 rutile phase (PDF No. 21-2176). While, another minor peak with 'o' corresponds to the MgO phase (PDF No. 45-0946). Therefore, in FIGURE 6, MgTiO_3 becomes the dominant phase. As a result, the MZT04 ceramic fabrication carried out in this study was proven to produce MgTiO_3 as the main phase, i.e. 87.02 – 90.55 % molar, and the remaining % is for TiO_2 and MgO minor phases (see TABLE 1). No peaks containing Zn were identified in FIGURE 6. This indicates that the mol fraction of Zn^{2+} ions have successfully entered the structure of Mg^{2+} ions to form a substitution solid solution (see Fig. 10 for an illustration of substitution solid solution and the explanation).

In FIGURE 7, the red line represents the calculated (model) diffraction pattern, the "+" symbol represents the measured (experimental) diffraction pattern, the blue vertical line under the diffraction pattern represents the Bragg peak belonging to all identified phases, namely MgTiO_3 , MgO , and TiO_2 . The green line shows the difference in intensity between the experimental and the model diffraction patterns. Figures of Merit (FoM) of the refinement consisting of the weighted factor (R_{wp}), experimental factor (R_{exp}), and the profile factor (R_{p}) are also shown. According to Ermawati [24], when the value of R_{p} , R_{wp} , and R_{exp} are less than 20% and the FoM index is less than 3% are the refinement has been successful and the output of the Rietveld refinement (i.e. data in TABLE 1) can be used for further analysis.

In TABLE 1, no extra phase of Zn_2TiO_4 was identified as reported by Ermawati in [27]. Therefore, the fabrication method reported in this study successfully to remove the Zn_2TiO_4 in the MZT04 ceramic system. The increased in sinter holding time expands the lattice

parameter size ($a=b$, c) in the MgTiO_3 phase, i.e. 5.057, 13.903 Å for 6 h; 5.058, 13.903 Å for 8 h; and 5.061, 13.914 Å for 10 h. This same trend was also detected in the unit cell volume size in the MgTiO_3 phase, i.e. (307.94 ± 0.08) Å³ for 6 h; (308.01 ± 0.08) Å³ for 8 h; and (308.94 ± 0.12) Å³ for 10 h.

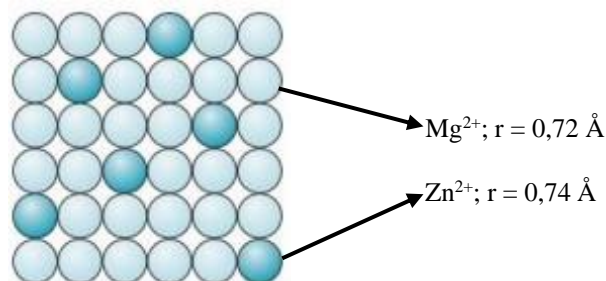


FIGURE 10. The substitution solid solution of the MZT04 ceramic [31].

In FIGURE 10, a regular expanse of spherical balls illustrates the position of Mg^{2+} ions in the MZT04 ceramic structure. Some of the Mg^{2+} ions are replaced by Zn^{2+} ions as dopant agent giving rise to a substitution solid solution. The Zn^{2+} ions were chosen based on several considerations, i.e. 1) to lower the formation temperature of the MgTiO_3 phase from 700°C (without Zn^{2+} ions addition) to 550 °C (with the addition of Zn^{2+} ions) [32]; 2) the Zn^{2+} ions have a fairly low melting point (420 °C [33]) as compared to the formation temperature of MgTiO_3 phase, i.e. (550°C [34]); 3) the Zn^{2+} and Mg^{2+} ions both have the same coordination number, i.e. octahedral so that there is no possibility for electrons to transfer (donor or acceptor) among the 2 ions so that the potential disturbance to the parent ceramic structure due to the addition of doping ions can be prevented [32]; and 4) the radius of Zn^{2+} ions is similar to that of Mg^{2+} ions, namely 0.72 Å (Mg^{2+} ions) and 0.74 Å (Zn^{2+} ions) [32]. However, the radius of Zn^{2+} ions are relatively larger than the radius of Mg^{2+} ions, therefore the presence of Zn^{2+} ions in the parent ceramic structure has the potential to increase the lattice parameter and the unit cell volume size of the parent (MgTiO_3) phase in the MZT04 ceramic (see TABLE 2).

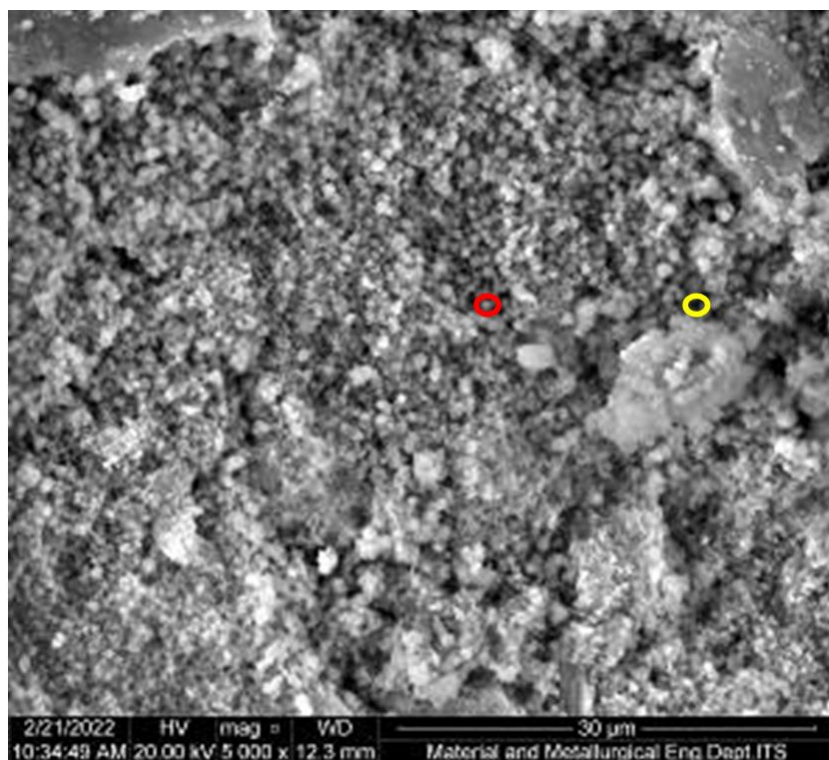
TABLE 2. The comparison of lattice parameters and unit cell volume of MgTiO_3 phase in PDF No. 06-494 database versus in MZT04 ceramics fabricated in this work.

Pure MgTiO_3 (PDF No. 06-494)			MgTiO_3 phase in MZT04 ceramics sintered at 1300 °C			
a=b (Å)	c (Å)	Unit cell volume (Å ³)	Sinter holding time (h)	a=b (Å)	c (Å)	Unit cell volume (Å ³)
5.054	13.899	(307.40)	6	5.057	13.900	(307.94 ± 0.08) Å
			8	5.058	13.904	(308.01 ± 0.08) Å
			10	5.061	13.914	(308.94 ± 0.12) Å

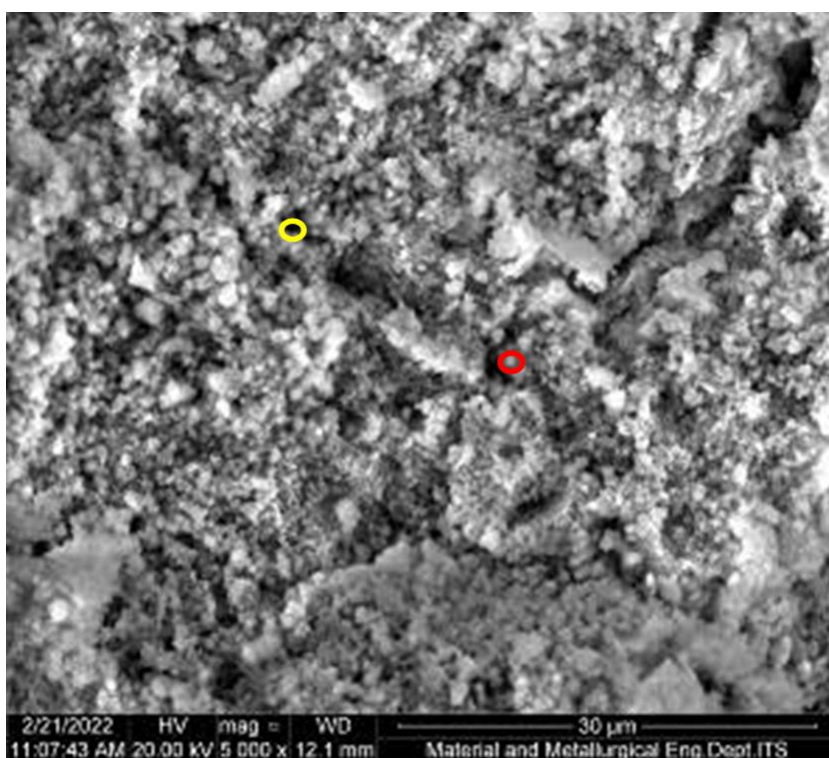
Based on TABLE 2, it is confirmed that the Zn^{2+} ions doping has increased the lattice parameter and unit cell volume size of the MgTiO_3 phase in the MZT04 ceramic system.

Microstructure and bulk density

FIGURE 11 shows the microstructure of the three MZT04 ceramics that was taken from a broken surface and measured using a scanning electron microscope (SEM) FEI inspects S50 with a magnification of 5000x and operating at 20 kV. FIGURE 12 shows the average diameter of the grains and pores that were measured using the ImageJ software as shown in FIGURE 4. FIGURE 13 shows the bulk density of MZT04 ceramics at the three-sintering holding time.

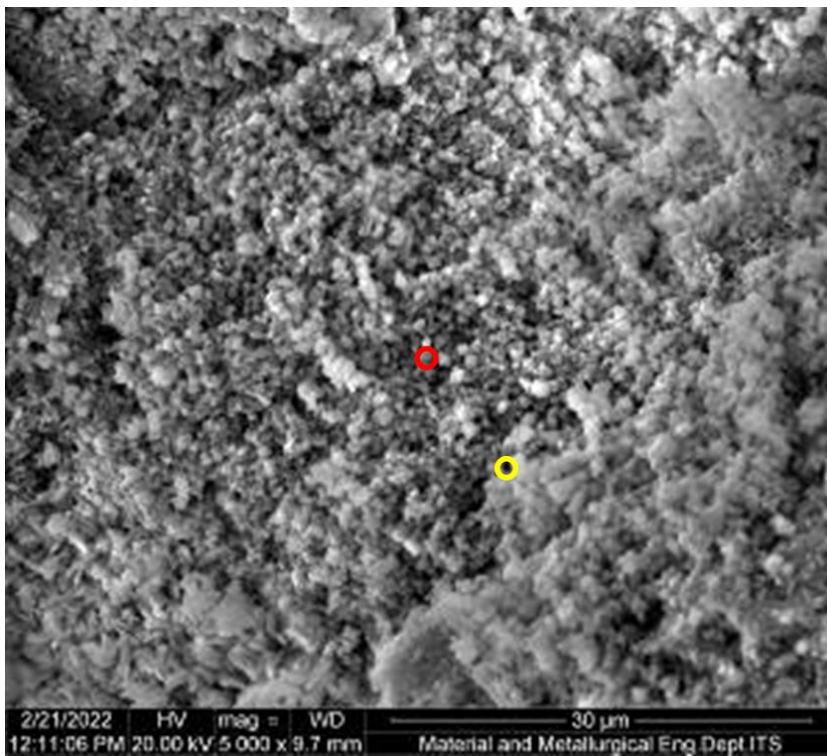


(a)



(b)

FIGURE 11. Microstructure of MZT04 ceramics with 5000x magnification after sintering for: (a) 6 h, (b) 8 h



(c)

FIGURE 11. Microstructure of MZT04 ceramics with 5000x magnification after sintering for: (c) 10 h (cont.).

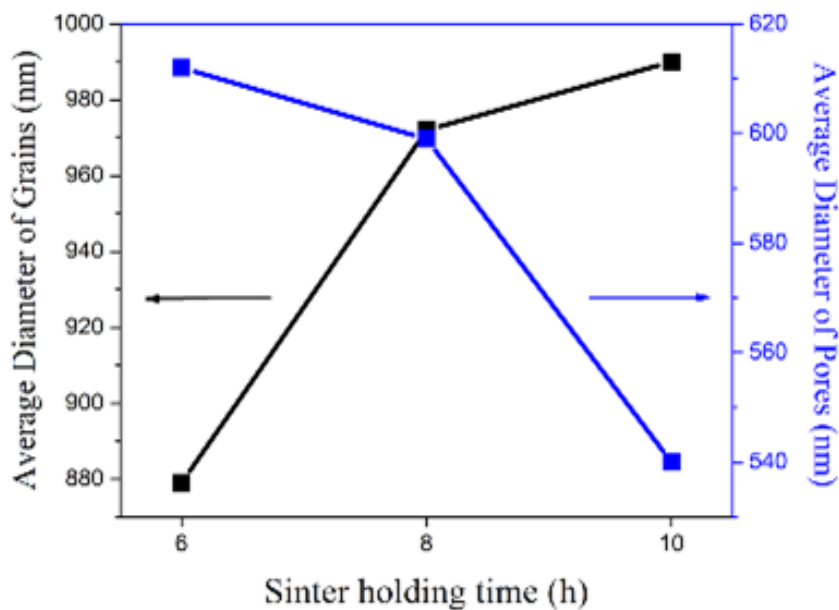


FIGURE 12. The average diameters of grains and pores of MZT04 ceramics with three variations of sinter holding time

In FIGURE 11, the surfaces of MZT04 ceramics are very dense and consists of grains (gray and white colors in the red circle) and pores (black in the yellow circle). The grains were not grown but they agglomerated. Using the ImageJ software, the grain and pore diameters were measured and plotted in FIGURE 12. As shown in FIGURE 12, the grains size increased from 879 nm (for 6 h), 972 nm (8 h), to 990 nm (10 h). Conversely, the average pores diameter

decreased from 612 nm (for 6 h), 599 nm (8 h), to 540 nm (10 h). Based on that, the increase in sintering holding time has enlarged the diameter of grain and reduced the size of the pores. The decrease in the pore size diameter has led to an increase in the bulk density of MZT04 ceramic (see FIGURE 13).

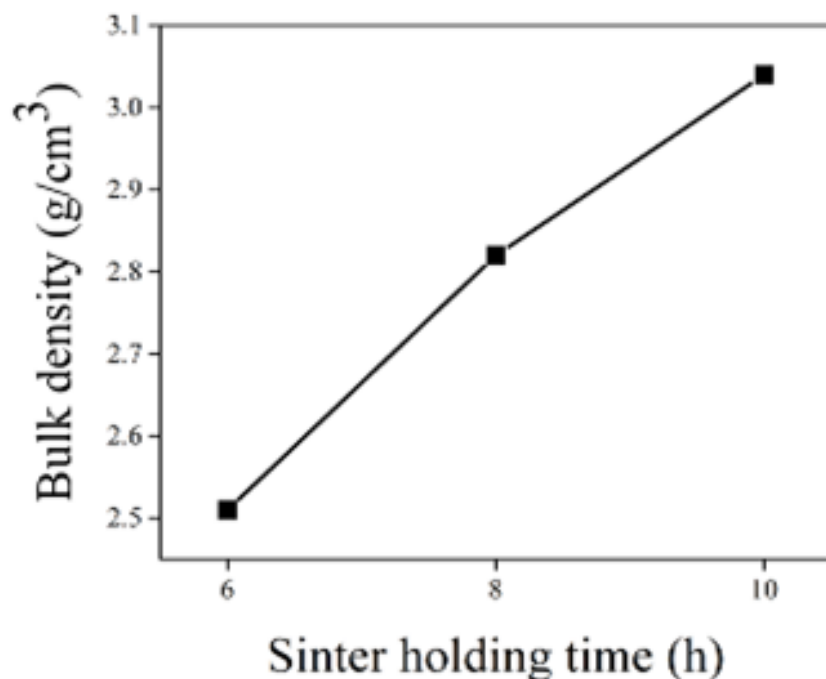


FIGURE 13. Bulk density of MZT04 ceramics as a function of sinter holding time

In FIGURE 13, bulk density of MZT04 ceramics increased from 2.51 g/cm³ (for 6 h), 2.82 g/cm³ (8 h), to 3.04 g/cm³ (10 h). Based on that, the increase in the sintering holding time affects the bulk density of MZT04 ceramics. Rettingtyas & Ermawati [35] reported that (Mg_{0.8}Zn_{0.2})TiO₃ ceramics sintered at 1100°C for 4, 6, and 8 h was able to produce higher bulk density, i.e. 3.382; 3.582; 3.667 g/cm³. Hence, the bulk density of MZT04 ceramics in this study is lower when compared to the bulk density of (Mg_{0.8}Zn_{0.2})TiO₃ ceramics reported by Rettingtyas & Ermawati [35]. A decreased bulk density of ceramics in this study might be related to the sinter holding time at high temperature as reported by Akmal & Ramlan [36] on Na-β-Al₂O₃ ceramics. Akmal & Ramlan explained that when the sinter holding time is increased, the pore size becomes larger because the gas needed to strengthen the bonds between atoms burns and evaporates which causes the density of the ceramic to decrease. However, the examination on this effect to the MZT04 ceramic systems has not been performed yet.

The resonance frequency and output power as DR material

FIGURE 14 shows the characterization of the resonant frequency and output power of the three MZT04 ceramics when the ceramic acts as a DR material in the DRO circuit as measured using a spectrum analyzer in the frequency range of 3-12 GHz with TE_{0,18} mode.

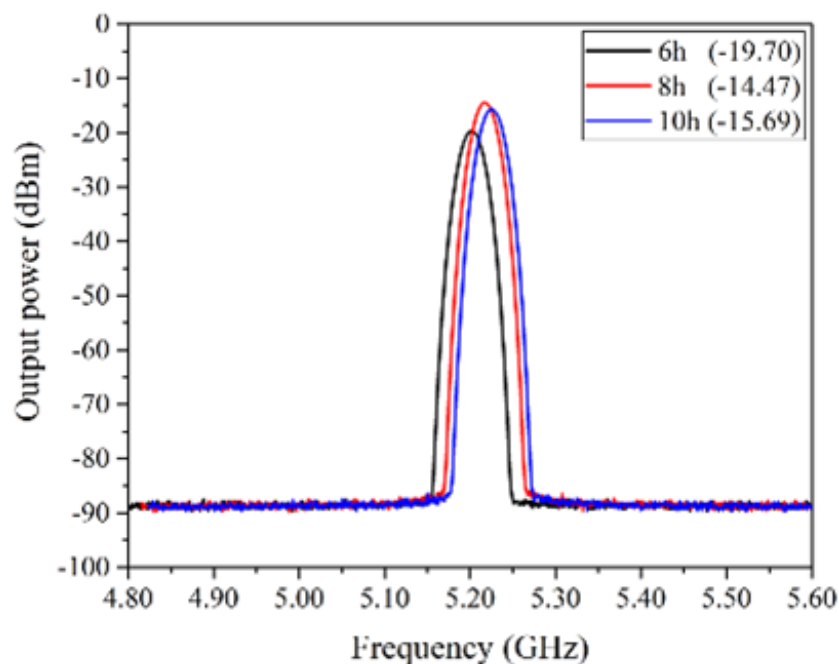


FIGURE 14. Resonant frequency signal of MZT04 ceramics as DR material in DRO circuit

In FIGURE 14, the position of peak resonant frequency is shifts slightly to the right as the sintering holding time increases, i.e 5.20 GHz (for 6 h) with the output power of -19.70 dBm; 5.21 GHz (8 h) with the output power of -14.47 dBm; and 5.22 GHz (10 h) with the output power of -15.69 dBm. This indicates that the increased sinter holding time has slightly shifted the peak of the resonant curve toward a higher frequency. In addition, the increase in sinter holding time also tends to cause the output power to be closer to zero, i.e. from -19.70, -14.47, to -15.69. The condition of the output power that is close to zero is desirable because it indicates that all parts of the ceramic have resonated at the same frequency. Data in FIGURE 14 confirmed that the three MZT04 ceramics fabricated in this work are capable of acting as resonator materials in the DRO circuit. FIGURE 15 shows the fitting of the resonant frequency curves in FIGURE 14 to the theoretical Gaussian curve in FIGURE 16.

In FIGURE 15, the full width at half maximum (FWHM) of the resonant frequency curve is 59.3 MHz (for 6 h), 61.6 MHz (8 h); and 61.2 MHz (10 h), see “w” values in the blue boxes. As seen, the FWHM of the resonant curve of the ceramics slightly increased with sinter holding time. In other word, the increase in sinter holding time causes the FWHM to increase. Izza & Ermawati in [18] that fabricated $(\text{Mg}_{1.0}\text{Zn}_{0.0})\text{TiO}_3$ ceramics reported the DR resonance frequencies of the ceramics were at 5.0-5.2 GHz. Meanwhile, Kadarosman & Ermawati in [21] that fabricated $(\text{Mg}_{0.9}\text{Zn}_{0.1})\text{TiO}_3$ ceramics reported the DR resonant frequencies was at 5.08-5.12 GHz. The DR resonance frequency in [18] and in [21] are similar to those in this work, but they did not measure the FWHM of the resonance frequency curves. All the results obtained in FIGURES 14 and 15 are the result of the similar structure and microstructure of the three MZT04 ceramics as well as the increase of bulk density along with increasing sinter holding time.

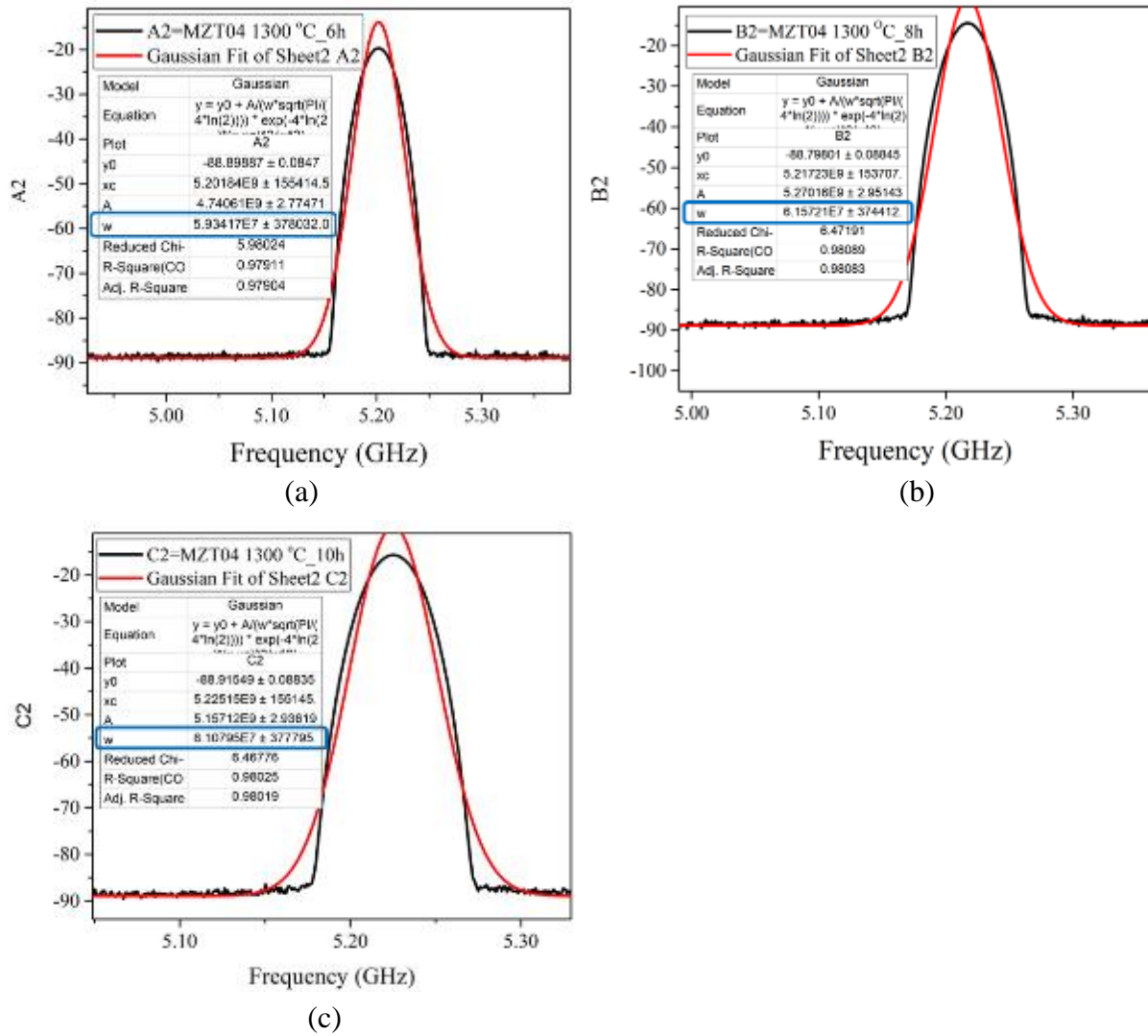


FIGURE 15. Fitting the MZT04 ceramic resonance frequency curves at sinter holding time of: (a) 6 h, (b) 8 h, (c) 10 h to the Gaussian curves. The “w” in blue boxes shows the FWHM of the curve.

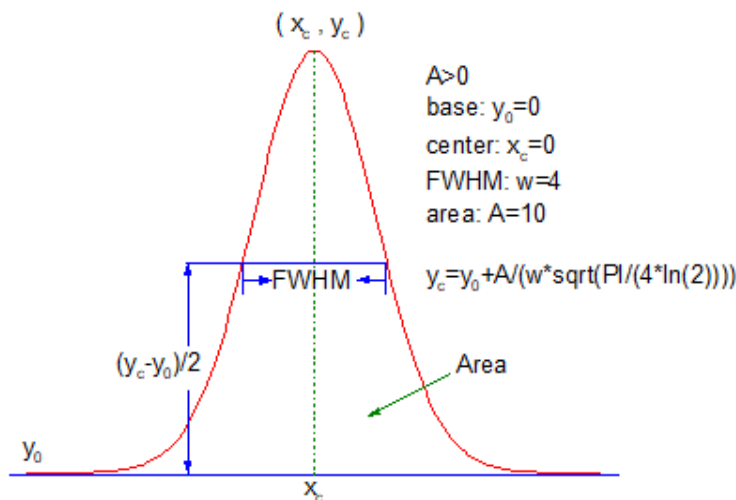


FIGURE 16. The theoretical Gaussian curve.

CONCLUSION

The work to fabricate and characterize MZT04 ceramics sintered at 1300°C by varying the holding time at 6, 8 and 10 h has been completed. The ceramic has MgTiO₃ as the main phase without accompanied by Zn₂TiO₄ at all. The microstructure of ceramics a very dense with increasing density along with the increase in sintering time, the three ceramics are also proven can be applied as a DR material in a DRO circuit because the ceramics are able to produce the resonant frequency signals at microwaves, especially at ~5.20 GHz with output power that is getting closer to zero along with an increase in sinter holding time from 6 to 8 h.

REFERENCES

- [1] S. Wu *et al.*, “Effect of Bi₂O₃ Additive on the Microstructure and Dielectric Properties of BaTiO₃ Based Ceramics Sintered at Lower Temperature,” *J. Mater. Sci. Technol.*, vol. 26, pp. 472-476, 2010, DOI: 10.1016/S1005-0302(10)60075-8.
- [2] M. Zhang *et al.*, “Structure and Properties Analysis for MgTiO₃ and (Mg_{0.97}M_{0.03})TiO₃ (M = Ni, Zn, Co, and Mn) Microwave Dielectric Materials,” *J. Alloys Compd.*, vol. 537, pp. 76-79, October 2012, DOI: 10.1016/j.jallcom.2012.05.026.
- [3] J. Zhang *et al.*, “MgTiO₃/TiO₂/MgTiO₃: An ultrahigh-Q and Temperature-stable Microwave Dielectric Ceramic Through Cofired Trilayer Architecture,” *Ceram. Int.*, vol. 44, no. 17, pp. 21000-21003, 2018, DOI: <https://doi.org/10.1016/j.ceramint.2018.08.135>.
- [4] Y. M. Miao *et al.*, “Low-temperature Synthesis of Nano-crystalline magnesium titanate materials by the sol-gel method,” *Mater. Sci. Eng. B*, vol. 128, no. 1, pp. 103-106, 2006, DOI: <https://doi.org/10.1016/j.mseb.2005.11.019>.
- [5] S. H. Lin, C. H. Shen and C. C. Ho, “Dielectric Performance and Physical Characterization of (Mg_{0.6}Zn_{0.4})_{0.95}Ni_{0.05}TiO₃ ceramics with ATiO₃ (A = Ca, Sr) Additions for Microwave Applications,” *J. Mater. Sci. Electron*, vol. 32, no. 23, pp. 27913-27922, 2021, DOI: 10.1007/s10854-021-07172-y.
- [6] Y. C. Liou and S. L. Yang, “Calcium-doped MgTiO₃-MgTi₂O₅ Ceramics Prepared using a Reaction-sintering Process,” *Mater. Sci. Eng. B*, vol. 142, no. 2, pp. 116-120, 2007, DOI: <https://doi.org/10.1016/j.mseb.2007.06.027>.
- [7] H. Wang *et al.*, “Sintering Behavior and Microwave Dielectric Properties of MgTiO₃ Ceramics Doped with B₂O₃ by Sol-Gel Method,” *J. Mater. Sci. Technol.*, vol. 28, no. 8, pp. 751-755, 2012, DOI: [https://doi.org/10.1016/S1005-0302\(12\)60125-X](https://doi.org/10.1016/S1005-0302(12)60125-X).
- [8] M. K. Suresh *et al.*, “Synthesis of Nanocrystalline Magnesium Titanate by an Auto-igniting Combustion Technique and its Structural, Spectroscopic and Dielectric Properties,” *Mater. Res. Bull.*, vol. 45, no. 7, pp. 761-765, 2010, DOI: <https://doi.org/10.1016/j.materresbull.2010.03.019>.
- [9] Y. F. Deng *et al.*, “Synthesis of Magnesium Titanate Nanocrystallites from a Cheap and Water-soluble Single-source Precursor,” *Inorganica Chim. Acta*, vol. 363, pp. 827-829, 2010, DOI: 10.1016/j.ica.2009.11.020.
- [10] N. Santha, M. Rakhi and S. Ganesanpotti, “Fabrication of High-quality Factor Cold Sintered MgTiO₃-NaCl Microwave Ceramic Composites,” *Mater. Chem. Phys.*, vol. 255, p. 123636, 2020, DOI: 10.1016/j.matchemphys.2020.123636.

- [11] I. Wibisono, "Perancangan Dielektrik Resonator Oscillator Untuk MOBILE WIMAX Pada Frekuensi 2,3 GHz Dengan Penambahan Coupling $\lambda/4$," 2010.
- [12] T. Firmansyah and G. Wibisono, "Penerapan Metode Monte-Carlo untuk Analisis Toleransi Perubahan Nilai Komponen Terhadap Kinerja Osilator Frekuensi 2,3 GHz," *J. Rekayasa Elektr.*, vol. 12, p. 92, 2017, doi: 10.17529/jre.v12i3.5564.
- [13] O. Kizilbey, O. Palamutcuogullari and B. S. Yarman, "Design of Low Phase Noise 7.7 GHz Dielectric Resonator Oscillator," *ELECO 2013 - 8th Int. Conf. Electr. Electron. Eng.*, pp. 591-594, November 2013, DOI: 10.1109/eleco.2013.6713914.
- [14] A. Warburton, "A Phase Tuned, Fixed Frequency Dielectric Resonator Oscillator Design," in *European Microwave Conference*, vol. 1, pp. 4, 2005, DOI: 10.1109/EUMC.2005.1608830.
- [15] J. Lee, Y. T. Lee and S. Nam, "A Phase Noise Reduction Technique in Microwave Oscillator using a High-Q Active Filter," *IEEE Microw. Wirel. Components Lett.*, vol. 12, pp. 426-428, 2002.
- [16] R. R. Jones and V. H. Estrick, "Low Phase Noise Dielectric Resonator Oscillator," *44th Annu. Symp. Freq. Control*, pp. 549-554, 1990.
- [17] N. Mahyuddin *et al.*, "Modeling of a 10GHz Dielectric Resonator Oscillator in ADS," 2006.
- [18] L. Izza and F. U. Ermawati, "Characterization of $(\text{Mg}_{1.0}\text{Zn}_{0.0})\text{TiO}_3+4 \text{ wt}\% \text{Bi}_2\text{O}_3$ Ceramics for Application as Resonator in Dielectric Resonator Oscillator Circuit," *J. ILMU Fis.*, Univ. ANDALAS, vol. 13, no. 2, pp. 62-69, Mar. 2021, DOI: 10.25077/jif.13.2.62-69.2021.
- [19] U. Frida *et al.*, "Blok Diagram Sirkuit DRO dan Blok Diagram Pengukuran Frekuensi Respon dan Daya Luaran DRO Pada C-Band untuk Keramik Dielektrik $(\text{Mg}_{1-x}\text{Zn}_x)\text{TiO}_3$," *Modul. Sertifikat Hak Cipta RI, No. Pencatatan 000203671 Tahun 2020*, 2020.
- [20] M. Jacob *et al.*, "Dielectric Characterization of Barium Fluoride at Cryogenic Temperatures using TE_{011} and Quasi TE_{0mn} Mode Dielectric Resonators," *Cryogenics (Guild)*, vol. 46, pp. 730-735, 2006, DOI 10.1016/j.cryogenics.2006.06.004.
- [21] A. Kadarosman and F. U. Ermawati, "The use of $(\text{Mg}_{0.9}\text{Zn}_{0.1})\text{TiO}_3+2\text{wt}\% \text{Bi}_2\text{O}_3$ Ceramics as a Dielectric Resonator Oscillator Material and Characterisation of Structure, Microstructure, and Density," *J. Neutrino*, vol. 13, no. 2, pp. 67-79, Jun. 2021, DOI: 10.18860/neu.v13i2.11720.
- [22] E. Ishida *et al.*, "Amorphous-Si Waveguide on a Garnet Magneto-optical Isolator with a TE Mode Nonreciprocal Phase Shift.," *Opt. Express*, vol. 25, no. 1, pp. 452-462, Jan. 2017, DOI: 10.1364/OE.25.000452.
- [23] L. Sánchez, S. Lechago and P. Sanchis, "Ultra-compact TE and TM Pass Polarizers Based on Vanadium Dioxide on Silicon.," *Opt. Lett.*, vol. 40, no. 7, pp. 1452-1455, Apr. 2015, DOI: 10.1364/OL.40.001452.
- [24] R. Yamaguchi, Y. Shoji and T. Mizumoto, "Low-loss Waveguide Optical Isolator with Tapered Mode Converter and Magneto-optical Phase Shifter for TE Mode Input," *Opt. Express*, vol. 26, no. 16, pp. 21271-21278, 2018, DOI: 10.1364/OE.26.021271.

- [25] Skyworks, "Properties, Test Methods, and Mounting of Dielectric Resonators," p. 2, 2017, [Online]. Available: https://cm-sitecore.skyworksinc.com/-/media/SkyWorks/Documents/Products/2501-2600/Properties_and_Mounting_of_Dielectric_Resonators_202803B.pdf. Retrieved February 11, 2020.
- [26] K. Wang *et al.*, "Solid-state Reaction Mechanism and Microwave Dielectric Properties of $0.95\text{MgTiO}_3-0.05\text{CaTiO}_3$ ceramics," *J. Mater. Sci. Mater. Electron.*, vol. 29, 2018, DOI: 10.1007/s10854-017-8111-z.
- [27] F. U. Ermawati *et al.*, "Preparation and Structural Study of $\text{Mg}_{1-x}\text{Zn}_x\text{TiO}_3$ Ceramics and their Dielectric Properties from 1 Hz to 7.7 GHz," *J. Mater. Sci. Mater. Electron.*, vol. 27, no. 7, pp. 6637-6645, 2016, DOI: 10.1007/s10854-016-4610-6.
- [28] V. G. Anugraha and Widyastuti, "Pengaruh Komposisi Sn dan Variasi Tekanan Kompaksi terhadap Densitas dan Kekerasan Komposit Cu-Sn untuk Aplikasi Proyektil Peluru Frangible dengan Metode Metalurgi Serbuk," *J. Tek. Pomits*, vol. 3, no. 1, pp. 102-107, 2014.
- [29] B. D. Cullity and S. R. Stock, "Elements of X-ray Diffraction," *Third Edition*, New York: Prentice-Hall, 2001.
- [30] F. U. Ermawati, "The Response of $(\text{Mg}_{0.6}\text{Zn}_{0.4})\text{TiO}_3$ Ceramic System as A Dielectric Resonator Oscillator at C-Band," *J. Phys. Conf. Ser.*, vol. 1805, no. 1, p. 12039, Mar. 2021, DOI: 10.1088/1742-6596/1805/1/012039.
- [31] R. S. Molla, "A study on Manufacturing of Deformed Bar (G 60-400W) at Elite Iron and Steel Industries." 2018, DOI: 10.13140/RG.2.2.24320.33289.
- [32] F. U. Ermawati, "Struktur Kristal Bahan Keramik," Surabaya: Unesa University Press, 2019.
- [33] Teck.com, "Zinc Metal Safety Data Sheet," *Trail*, British Columbia, 2018. [Online]. Available: <https://www.teck.com/media/Zinc-Metal-2018-SDS-.pdf>.
- [34] F. Z. Teng, "Magnesium," in *Encyclopedia of Earth Sciences Series*, pp. 853-856, 2018.
- [35] N. Rettiningtyas and F. U. Ermawati, "Sintesis dan Fabrikasi Keramik $(\text{Mg}_{0.8}\text{Zn}_{0.2})\text{TiO}_3 + 2 \text{ wt}\% \text{ Bi}_2\text{O}_3$ Sebagai Bahan Dielektrik Serta Karakterisasi Struktur dan Densitasnya Akibat Variasi Waktu Tahan Sinter," *Inov. Fis. Indones.*, vol. 9, pp. 25-33, 2020, [Online]. Available: <https://jurnalmahasiswa.unesa.ac.id/index.php/6/article/view/33811>.
- [36] A. Johan and R. Ramlan, "Karakterisasi Konduktivitas, Porositas dan Densitas Bahan Keramik Na- β - Al_2O_3 dari Komposisi Na_2O 13% dan Al_2O_3 87% dengan Variasi Waktu Penahanan," *J. Penelit. Sains*, vol. 11, no. 3, 2008, doi: 10.36706/jps.v11i3.395.